# Spatial Pattern Investigation of Olivine on Mars using OMEGA and MOLA Remote Sensing Data: A Case Study at Valles Marineris and Nili Fossae

Leilei Jiao[1] , Yusheng Xu[1,2], Rong Huang[1,2], Zhen Ye[1,2], Sicong Liu[1,2], Shijie Liu[1,2], Xiaohua Tong[1,2]

[1]College of Surveying and Geoinformatics, Tongji University, Shanghai, China - yusheng_xu@tongji.edu.cn
[2] Shanghai Key Laboratory for Planetary Mapping and Remote Sensing for Deep Space Exploration, Shanghai, China

**Keywords:** Olivine, Spatial pattern, Kernel density estimation, Bivariate spatial autocorrelation.

**Abstract:**

Olivine is a mineral indicative of water activity in the mantle, and its presence can elucidate the petrological evolution and history of magmatic igneous rocks. In this work, we conducted a preliminary investigation into the characteristics and patterns of the spatial relationships between representative Martian mineral (i.e., olivine) and geomorphic features, aiming to provide geographical insights into the potential habitable environment of Mars. Specifically, an analytical framework is constructed to explore the spatial connection between hydrated minerals like olivine and topographic features regarding the relationship between environmental factors and mineral distributions. Furthermore, an analytical paradigm for responding to the spatial relationship is established. The spatial distribution pattern of olivine in Valles Marineris and Nili Fossae on Mars is depicted using kernel density analysis and bivariate spatial autocorrelation models. Based on this, the coupling relationship between olivine and environmental factors is constructed to quantify the strength of the link, and the interaction mechanism between olivine and geomorphological terrain is identified. The study results demonstrate that the distribution of olivine exhibits pronounced spatial clustering characteristics. Furthermore, the spatial distribution pattern of olivine and topographic features displays elevation differentiation characteristics. In the study region, topographic features dominate the spatial differentiation of olivine, specifically within the context of Valles Marineris. The spatial linkage strengths between the factors in the area vary considerably.

## 1. Introduction

Many hydrated minerals on Mars are formed through weathering, sedimentation, and hydrothermal processes on the surface or underground (Gainey et al., 2017). These minerals record the history of water-rock interactions on Mars, and their types, abundance, and distribution can provide information on the geological evolution process and related ancient environment of Mars, as well as the livability of Martian past life (Baker, 2001). Early impacts and thermal alteration were hypothesized to transform the olivine bedrock into clay. This transformation may be evidence of past liquid water on Mars (The Omega Team et al., 2005). Besides, olivine may be a more reliable indicator of water activity and water-rich conditions in the mantle. Therefore, a comprehensive understanding of olivine in mantle minerals on Mars is helpful to gain insight into past and future aspects of the Earth (Peslier, 2010). Studying the distribution patterns of olivine on Mars is essential for explaining the planet's environment and evolution over time, which in turn plays a vital role in unraveling the mysteries surrounding the origin and early development of life. Furthermore, the data obtained from mineral research is crucial for planning and preparing future missions to Mars and enhancing our understanding of the potential for life outside of Earth (Wernicke and Jakosky, 2021).

Among all the influential factors, terrain, as a non-zonal factor, can indirectly affect the distribution pattern and characteristics of minerals through changes in land cover (Foley et al., 1996). Mars's morphology is complex, and its landform directly or indirectly affects the distribution of minerals on Mars (Ehlmann et al., 2011), so understanding the regional distribution and formation mechanisms of Martian minerals is necessary to understand the habitable conditions for the development of life on Mars (Tosca et al., 2008). The potential for life beyond Earth is intimately linked to Mars's history and distribution of water and minerals (Du et al., 2023). Previous studies on Martian minerals have concentrated on the detection and general characterization of minerals, with little attention paid to the multiple pathways by which they are formed. Sediments are generated, transported, and lithified by various mechanisms, including episodic floods, subsurface hydrothermal circulation, and significant impacts (Sheppard et al., 2021). These processes result in the formation of landforms, such as channels, mons, and plateaus. Topographic mapping provides technical support for studying Mars landing zone selection and geological evolution (Liu and Cheng, 2023). However, analyses of Martian minerals have mainly involved the interpretation of their morphology and composition (Rogers and Hamilton, 2015), which is insufficient for our understanding of the spatial characteristics of Martian minerals and their mechanisms of formation. Investigating the distribution and influencing factors of minerals on Mars is necessary.

Currently, there is limited work on the distribution patterns of Martian minerals, and research on the key factors driving quantitative measurements of mineral distribution in different regions is relatively scarce. For example, spatial analysis based on geographic data has laid the foundation for conducting geographical research on Martian mineral distribution (Anselin, 1995). The spatial analysis model can fully characterize the Spatial correlations and heterogeneity of geographic objects and objectively reflect the relationships between various elements in local space (Foley et al., 1996). Studying the distribution mechanism of minerals on Mars and their relationship with landforms can aid in understanding the evolution of early life and habitats in synchrony on Earth and the hunt for potential life on Mars (Bosak et al., 2021).

OMEGA-based global maps of various mineral species including olivine has been reported in the previous published. Here we present a detailed analysis of the spatial distribution and the complex and varied landforms of olivine on Mars. Studying spatial models formed by the interaction between spatial

elements of minerals like olivine and geomorphology is important. It is essential to explore the potential relationship between minerals and geomorphology. Our contribution lies in (1) identifying the spatial characteristics of olivine distribution on Mars to establish a basis for differentiating between minerals and (2) conducting spatial autocorrelation research based on the correlation between environmental factors and olivine spatial distribution. The objective is to preliminarily explore the mechanism of uneven mineral spatial distribution and enrich our understanding of the connotation of Martian minerals, providing geographical references for future exploration.

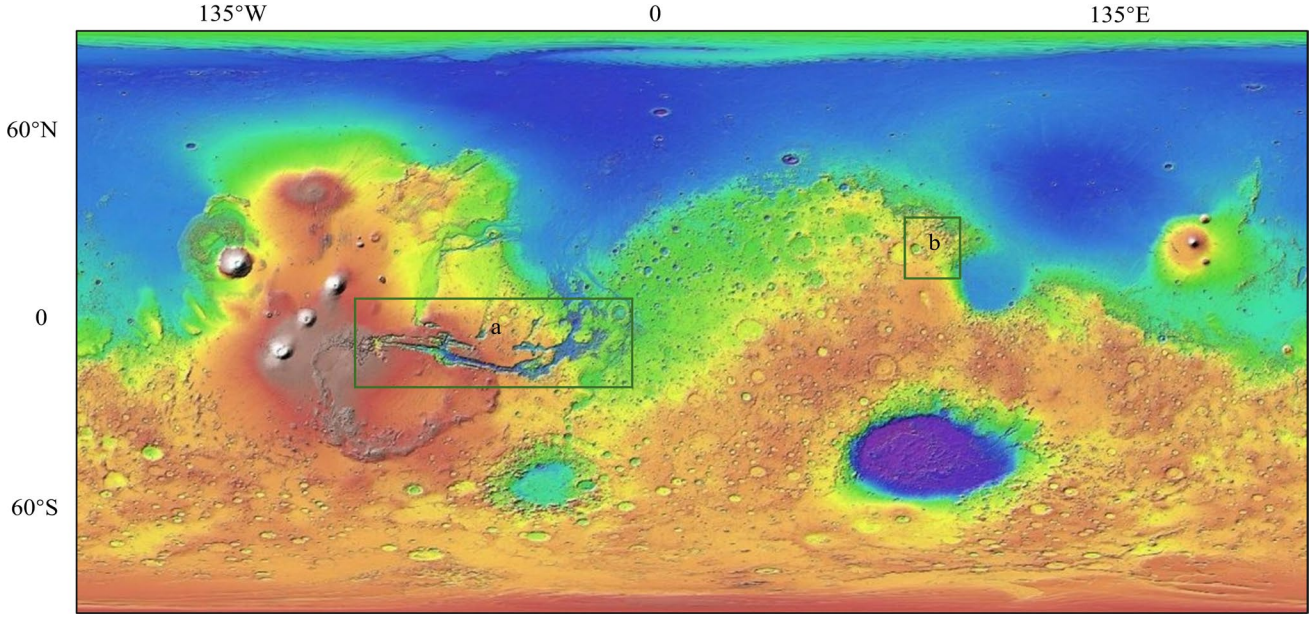


Figure 1. Our investigation area: (a) Valles Marineris and (b) Nili Fossae. (MOLA maps courtesy of NASA/Goddard Goddard Space Flight Center)

## 2. Study area and data sets

### 2.1 Study area

The presence and size of Martian outflow systems provide the most compelling evidence for a hydrological cycle and large amounts of water on Mars, respectively (Lunine et al., 2003). Valles Marineris is situated on the Tharsis Rise, representing Mars's youngest tectonic province. Valles Marineris offers unparalleled opportunities to study surface morphology, providing invaluable insights into the environmental conditions that once prevailed on Mars (Watkins et al., 2020). The Nili Fossae is a group of concentric grabens situated along the north-western border of the Isidis impact basin. Its distinctive surface formations and water-altered sediments suggest that the region was historically characterized by a diverse array of volcanic lava and multi-stage water-altered processes (Ehlmann et al., 2009). Valles Marineris and Nili Fossae, considered to be a flood channel for water to flow out, display evidence of mineralogical deposits that were formed as a consequence of aqueous alteration during the geological past (Hoefen et al., 2003; S. Murchie et al., 2009; Stähler et al., 2022). Prior research has also demonstrated that the fluvial process was a primary driver in the formation of the channel and its surrounding area, resulting in the development of a diverse range of minerals (Gendrin et al., 2005; S. L. Murchie et al., 2009)

### 2.2 Testing datasets

**2.2.1 Mineral data:** OMEGA is a visible and near-infrared (VNIR) imaging spectrometer onboard the Mars Express. It covers the wavelength range of 0.35 to 5.1μm. In this paper, the OMEGA targeted mode observation with a spatial resolution of 0.3–4.8 km/pixel (Poulet et al., 2007).

The OMEGA image (https://ode.rsl.wustl.edu/) can better constrain the geological background and provide extensive and gain coefficients were employed to transform the uncalibrated coverage for this study. A linear conversion formula and offset DN image into a radiance-valued image. This process obtained global distribution maps of olivine (Ody et al., 2012).

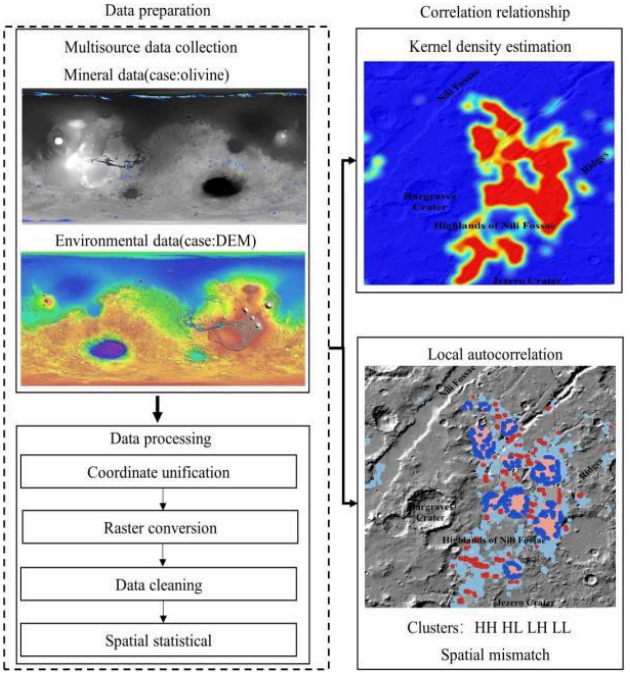


Figure 2. Framework of this study.

**2.2.2 Environmental data:** Considering data availability and relevance to olivine, we collected two types of data: terrain data and thermophysical property data. The topography of the study area was depicted using digital elevation model data, which is not subject to limitations imposed by light and darkness. This data provides a realistic representation of the morphological features of the landscape. Mars MGS MOLA DEM data (https://astrogeology.usgs.gov/) were selected to extract factors representing topographic features, and Elevation, Aspect, Slope, Shade, and Relief data were obtained at appropriate resolutions to explain the spatial differences in the spatial patterns of minerals in different landscape types. Albedo and thermal inertia are crucial factors in land surface physical processes. Global albedo maps provide evidence of aeolian sediment transport and/or surface dust deposition/erosion in regional areas (Rice et al., 2018). The Global Thermal Inertia map provides an in-depth view of the physical nature of the Martian landscape in terms of factors such as grain scale, degree of consolidation, rock richness, and bedrock exposure (Presley and Christensen, 1997). The data obtained from Mars Orbital Data Explorer provide information on the complexity of the surface (albedo data) and the vertical and horizontal properties of the surface materials (thermal inertia data, TI).

## 3. Method

The preliminary study comprised a comprehensive analysis of the selected environmental factors, using the CRITIC method to ensure the environmental data were as objective and scientifically robust as possible. Spatial patterns of olivine were revealed through kernel density estimation. Then, spatial statistics were employed to derive key independent and causal indicators, which were subsequently used in the analysis. Finally, local Moran was employed to quantify the strength of the spatial associations between olivine and environmental factors. The spatial geographic pattern of Martian olivine in the specified exposure area was illustrated by utilizing spatial autocorrelation and kernel density analyses. The prevailing factors underlying olivine geographic differentiation were then quantified, and the interaction mechanism between olivine and the geographic environment was preliminarily explored. The framework of this study is shown in Figure 2.

### 3.1 CRITIC method

The CRITIC method is based on the comparative strength of the evaluation indicators and the conflict between the indicators to measure the weight of the indicators comprehensively. Compared with subjective methods, CRITIC method is more objective and scientific, and compared with the entropy weighting method, which determines the weights based on the degree of dispersion of the indicator data, the results of the CRITIC method are more robust (Diakoulaki et al., 1995).

$$S_j = \sqrt{\frac{\sum_{i=1}^{p} x_{ij}}{q-1}}, R_j = \sum_{i=1}^{q} (1 - r_{ij})$$
$$C_j = S_j \times R_j$$
$$W_j = C_j / \sum_{j=1}^{q} C_j \qquad (1)$$
$$U_i = \sum_{j=1}^{q} x_{ij} W_j$$

Where $p$ is the number of datasets, $q$ is evaluation indicators, the variable $x_{ij}$ denotes the value of the $j$ evaluation indicator for the $i$ sample of the mineral after dimensionless processing. The value of the $j$ evaluation index of the $i$ sample after the aforementioned processing is represented by $S_j$. The variable $r_{ij}$ denotes the correlation coefficient between the evaluation indexes $i$ and $j$. $C_j$ denotes the amount of information conveyed by the $j$ evaluation index. The greater the value of $C_j$, the more significant the role of the $j$ evaluation index within the overall system of evaluation indexes, and the greater the weight assigned to it. $U_i$ denotes the value of the $i$ composite index of olivine.

### 3.2 Identification of olivine patterns using KDE

Kernel density estimation (KDE) represents a pivotal approach to investigating the aggregation zone of polycentric structures in olivine. This method enables the continuous simulation of spatial point element distribution density, thereby facilitating the effective excavation of the aggregation zone of various types of elements (Amador et al., 2018). The distribution density of the olivine is determined by moving the cell to simulate the spatial distribution of the elemental object in question.

$$f(x,y) = \frac{1}{nh^2} \sum_{i=1} K\left(\frac{d_i}{h}\right) \qquad (2)$$

Where $f(x,y)$is the density estimation at location $(x,y)$, $n$ is the number of olivines, $h$ is the search radium, $d_i$ is the distance between the olivine $x$ and $y$, and the $i_{th}$ observations of olivine and $K$ is the kernel function.

### 3.3 Local Moran's I indicators

Moran's I indicates the level of spatial autocorrelation at the different spatial scales. Local Moran which measures whether there is a local spatial similarity or heterogeneity between an observation at each spatial location and the surrounding neighbouring observations.

$$I = \frac{\sum_m \left(\sum_n w_{mn} z_n^l \times z_m^k\right)}{\sum_n \left(z_m^k\right)^2} \qquad (3)$$

Here $I$ is Moran's I statistic, $z_n^l$ represents the deviation of variable $l$ from its mean value at observation $n$ . $z_m^k$ is the deviation value of variable $k$ from its mean at observation $m$ .

The local Moran Indicators of Spatial Association analysis can help us comprehend a variable's spatial patterns of high and low values within a specific geographical area. Through quantifying the degree of clustering, we identified specific spatial clusters that displayed a spatial incongruence between minerals and environmental factors. Compared to other geospatial approaches, local Moran's I enabled the identification of statistically significant spatial clusters by comparing individual locations with neighboring samples.

## 4. Results

### 4.1Spatial olivine distribution

Kernel density estimation provides an objective means of analysing the aggregation characteristics and ductility of olivine. The results of the kernel density analysis of the spatial location information of olivine indicate that the overall distribution characteristics of olivine are extensive, while the

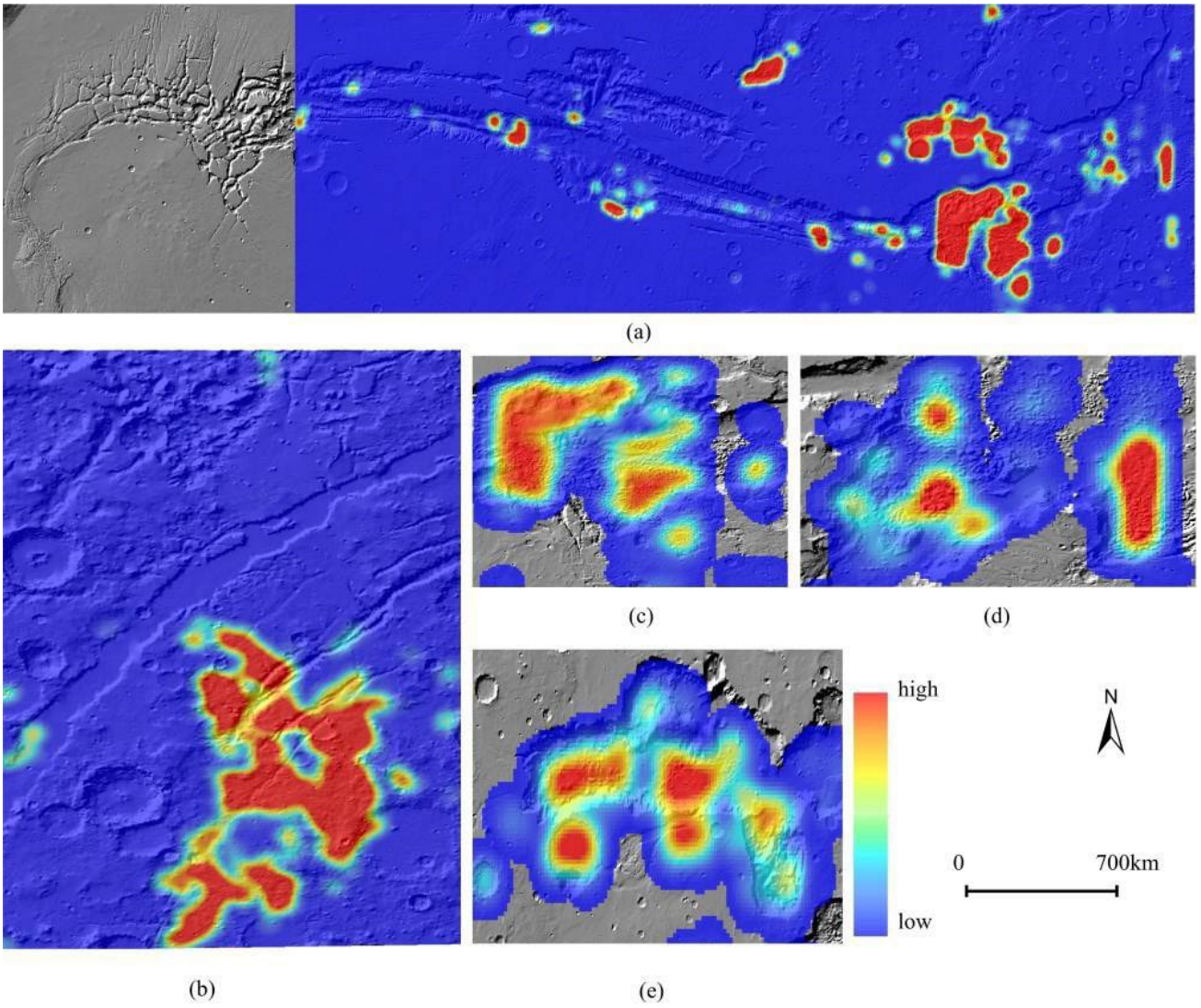


Figure 3. Spatial distribution of olivine in selected areas: (a) kernel density estimation results of Valles Marineris; (b) kernel density estimation results of Nili Fossae; (c) kernel density estimation results of Capri Chasma, (d) Ganges Chasma and (e) Eos Chasma on the Estern Flank.

overall spatial concentration characteristics are not balanced. There are significant zonal variations in the overall spatial distribution of the olivine in Valles Marineris. The western flank exhibits the lowest density of olivine distribution, followed by the central flank, with the highest density observed in the eastern flank. The spatial distribution of olivine in study area is characterised by a high degree of concentration, exhibiting the distribution patterns of "block concentration and scattered distribution". In the example of the Valles Marineris, the eastern flank represents the longest segment of the Valles Marineris province, which consists of five distinct area: Coprates Chasma, Capri Chasma, Eos Chasma, Ganges Chasma and Juventae Chasma. The common features of the terrain in this area are crater, landslide and yardang. Figure 3 shows that the distribution of olivine in Capri Chasma, Ganges Chasma and Eos Chasma on the eastern flank is more concentrated and widespread, while in other areas the distribution is less concentrated and more dispersed.

### 4.2 Spatial olivine distribution

We used Moran's I statistics to measure olivine's overall degree of spatial autocorrelation. Moreover, local spatial autocorrelation facilitated the delineation of concrete spatial clusters pertaining to spatial autocorrelation, thereby enabling us to discern the spatial mismatch in the minerals on Valles Mariner is and Nili Fossae. Figure 4 depicts the spatial clusters identified in study area through univariate analyses of local spatial autocorrelation. From the results of the univariate local spatial autocorrelation of the olivine in Valles Marineris, we observed that the low-low clusters were mainly distributed, and the low-high clusters and high-low clusters were distributed primarily on the eastern flank. These two types of clusters were prevalent in all valleys; however, only Noctis Labrynthus lacked low-low clusters. With regard to the mismatched spatial clusters (high-low and low-high), all Valles Marineris have low-low clusters, and the clusters were primarily located in the central flank and eastern flank, which might have been related to factors such as topographical variables. The coverage of clustered areas in all areas except Noctis Labrynthus was relatively low, and Ophir Chasma had the lowest coverage, showing weaker spatial agglomeration.

In marked contrast to the local spatial autocorrelation of olivine, we found only three types of spatial clusters concerning the local spatial autocorrelation in Valles Marineris: high-low, low-high and low-low. We found that large contiguous areas on Valles Marineris characterized the low-low clusters. Aside from

Coprates Chasma, the areas in which the low-high clusters of the eastern flank were distributed were an extension of the low-high and high-high clusters of the olivine.

Figure 5 illustrates the outcomes of the bivariate spatial autocorrelation analysis, which indicate that the spatial distribution of olivine in Valles Marineris and Nili Fossae is significantly correlated with the elevation factor. Moreover, the elevation is negatively correlated with olivine, exhibiting the highest degree of spatial autocorrelation. The value of Moran's I is -0.16 and 0.1, which indicates that the most responsive surface characteristics of Valles Marineris and Nili Fossae are the changes in elevation. This can be employed to inform estimates for the spatial evolution of the olivine. It can be hypothesised that alterations in elevation may precipitate shifts in the spatial distribution pattern of olivine.

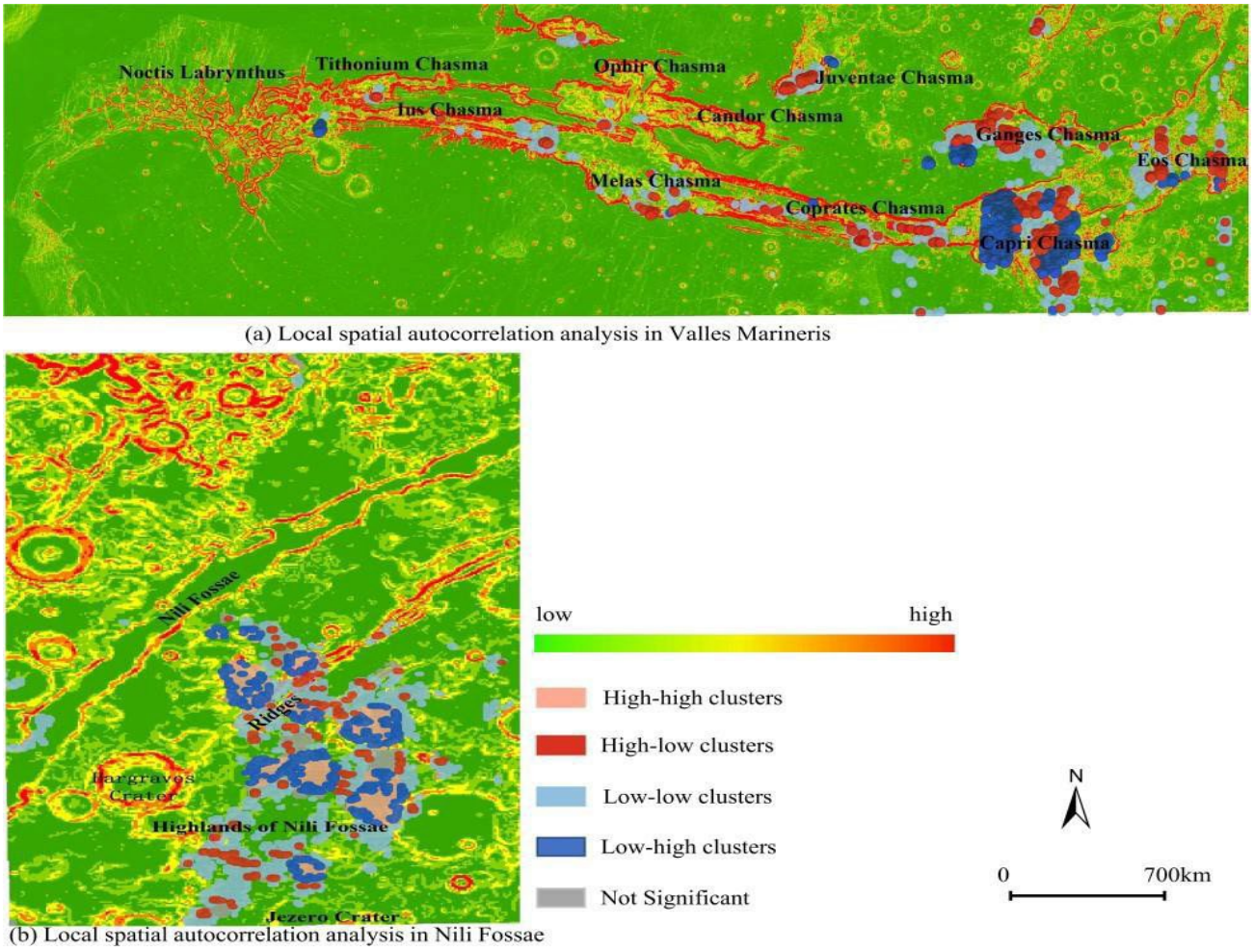


Figure 4. Univariate local spatial autocorrelation (local Moran Indicators) analysis of olivine

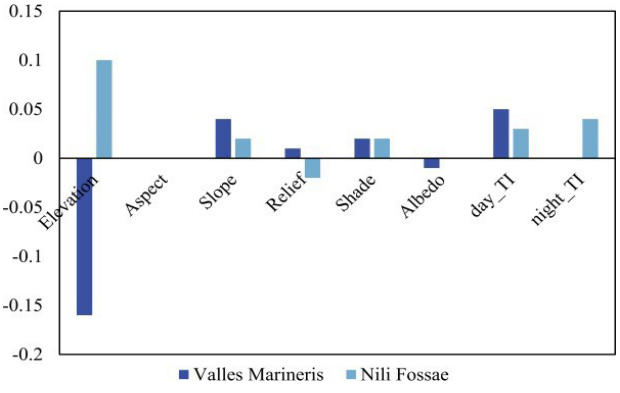


Figure 5. Bivariate local spatial autocorrelation results of olivine

## 3. Conclusion

This paper analyses the spatial relationships of representative Martian hydrated mineral (i.e., olivine) in Valles Marineris and Nili Fossae on Mars. It constructs an analytical framework based on the coupling relationship between topography and olivine. The framework tried to redefine the spatial distribution pattern of olivine, revealing the interrelationship between olivine and topography with the help of KDE and Moran models. This paper presents a novel interpretation of the spatial distribution of olivine in Valles Marineris and Nili Fossae, emphasizing the external landform topographic features. These include the distribution of olivine in different landforms, which exhibits a typical contiguous distribution and a spreading pattern along the line. Furthermore, the paper indicates that the spatial correlation of the spatial distribution of olivine with the elevation factor is -0.16 on

Vallies Marineris and 0.1 on Nili Fossae. This represents the most significant correlation observed among the environmental factors. These findings corroborate the hypothesis that the regional terrain significantly influences the distribution of olivine in the Valles Marineris and Nili Fossae (Mandon et al., 2020; Noe Dobrea et al., 2008). Furthermore, these findings have significant theoretical implications for understanding the regional distribution of olivine, which could provide a reference point for investigating potential habitable environments on Mars.

We also explored the spatial differentiation and driving mechanisms of mineral distribution on Mars at multiple regional scales. It fills gaps in large-scale analysis research and provides a geographical basis for the comprehensive and systematic interpretation mechanisms and future Mars exploration implementation.

## Acknowledgements

The work described in this paper was supported by the National Key R&D Program of China (2022YFF0504100).

## References

Amador, E.S., Bandfield, J.L., Thomas, N.H., 2018. A search for minerals associated with serpentinization across Mars using CRISM spectral data. Icarus 311, pp.113–134.

Anselin, L., 1995. Local Indicators of Spatial Association—LISA. Geographical Analysis 27, pp.93–115.

Baker, V.R., 2001. Water and the martian landscape. Nature 412, pp. 228–236.

Bosak, T., Moore, K.R., Gong, J., Grotzinger, J.P., 2021. Searching for biosignatures in sedimentary rocks from early Earth and Mars. Nat Rev Earth Environ 2, pp.490–506.

Diakoulaki, D., Mavrotas, G., Papayannakis, L., 1995. Determining objective weights in multiple criteria problems: The critic method. Computers & Operations Research 22, pp.763– 770.

Du, P., Yuan, P., Liu, J., Ye, B., 2023. Clay minerals on Mars: An up-to-date review with future perspectives. Earth-Science Reviews 243, pp.104491.

Ehlmann, B.L., Mustard, J.F., Murchie, S.L., Bibring, J.-P., Meunier, A., Fraeman, A.A., Langevin, Y., 2011. Subsurface water and clay mineral formation during the early history of Mars. Nature 479, pp.53–60.

Ehlmann, B.L., Mustard, J.F., Swayze, G.A., Clark, R.N., Bishop, J.L., Poulet, F., Des Marais, D.J., Roach, L.H., Milliken, R.E., Wray, J.J., Barnouin-Jha, O., Murchie, S.L., 2009. Identification of hydrated silicate minerals on Mars using MRO-CRISM: Geologic context near Nili Fossae and implications for aqueous alteration. J. Geophys. Res. 14.E2 (2009).

Foley, J.A., Prentice, I.C., Ramankutty, N., Levis, S., Pollard, D., Sitch, S., Haxeltine, A., 1996. An integrated biosphere model of land surface processes, terrestrial carbon balance, and vegetation dynamics. Global Biogeochemical Cycles 10, pp.603–628.

Gainey, S.R., Hausrath, E.M., Adcock, C.T., Tschauner, O., Hurowitz, J.A., Ehlmann, B.L., Xiao, Y., Bartlett, C.L., 2017. Clay mineral formation under oxidized conditions and implications for paleoenvironments and organic preservation on Mars. Nat Commun 8, pp.1230.

Gendrin, A., Mangold, N., Bibring, J.-P., Langevin, Y., Gondet, B., Poulet, F., Bonello, G., Quantin, C., Mustard, J., Arvidson, R., LeMouélic, S., 2005. Sulfates in Martian Layered Terrains: The OMEGA/Mars Express View. Science 307, pp.1587–1591.

Hoefen, T.M., Clark, R.N., Bandfield, J.L., Smith, M.D., Pearl, J.C., Christensen, P.R., 2003. Discovery of Olivine in the Nili Fossae Region of Mars. Science 302, pp.627–630.

Liu, D., Cheng, W., 2023. Progress and prospects for research on Martian topographic features and typical landform identification. Front. Astron. Space Sci. 10, pp.1275516.

Lunine, J.I., Chambers, J., Morbidelli, A., Leshin, L.A., 2003. The origin of water on Mars. Icarus 165, pp.1–8.

Mandon, L., et al. "Refining the age, emplacement and alteration scenarios of the olivine-rich unit in the Nili Fossae region, Mars." Icarus 336, pp.113436.

Murchie, S., Roach, L., Seelos, F., Milliken, R., Mustard, J., Arvidson, R., Wiseman, S., Lichtenberg, K., Andrews-Hanna, J., Bishop, J., Bibring, J., Parente, M., Morris, R., 2009. Evidence for the origin of layered deposits in Candor Chasma, Mars, from mineral composition and hydrologic modeling. J. Geophys. Res. 114.E2 (2009).

Murchie, S.L., Mustard, J.F., Ehlmann, B.L., Milliken, R.E., Bishop, J.L., McKeown, N.K., Noe Dobrea, E.Z., Seelos, F.P., Buczkowski, D.L., Wiseman, S.M., Arvidson, R.E., Wray, J.J., Swayze, G., Clark, R.N., Des Marais, D.J., McEwen, A.S., Bibring, J., 2009. A synthesis of Martian aqueous mineralogy after 1 Mars year of observations from the Mars Reconnaissance Orbiter. J. Geophys. Res. 114.E2 (2009).

Noe Dobrea, E.Z., Poulet, F., Malin, M.C., 2008. Correlations between hematite and sulfates in the chaotic terrain east of Valles Marineris. Icarus 193, pp.516–534.

Ody, A., Poulet, F., Langevin, Y., Bibring, J. -P., Bellucci, G., Altieri, F., Gondet, B., Vincendon, M., Carter, J., Manaud, N., 2012. Global maps of anhydrous minerals at the surface of Mars from OMEGA/MEx. J. Geophys. Res. 117.E11 (2012).

Peslier, Anne H. "A review of water contents of nominally anhydrous natural minerals in the mantles of Earth, Mars and the Moon." Journal of Volcanology and Geothermal Research 197.1-4 (2010), pp. 239-258.

Poulet, F., Gomez, C., Bibring, J. -P., Langevin, Y., Gondet, B., Pinet, P., Belluci, G., Mustard, J., 2007. Martian surface mineralogy from Observatoire pour la Minéralogie, l'Eau, les Glaces et l'Activité on board the Mars Express spacecraft (OMEGA/MEx): Global mineral maps. J. Geophys. Res. 112.E8 (2007).

Presley, M.A., Christensen, P.R., 1997. Thermal conductivity measurements of particulate materials 1. A review. J. Geophys. Res. 102, pp.6535–6549.

Rice, M.S., Reynolds, M., Studer-Ellis, G., Bell, J.F., Johnson, J.R., Herkenhoff, K.E., Wellington, D., Kinch, K.M., 2018. The albedo of Mars: Six Mars years of observations from Pancam on the Mars Exploration Rovers and comparisons to MOC, CTX and HiRISE. Icarus 314, pp.159–174.

Rogers, A.D., Hamilton, V.E., 2015. Compositional provinces of Mars from statistical analyses of TES, GRS, OMEGA and CRISM data. JGR Planets 120, pp.62–91.

Sheppard, R.Y., Thorpe, M.T., Fraeman, A.A., Fox, V.K., Milliken, R.E., 2021. Merging Perspectives on Secondary Minerals on Mars: A Review of Ancient Water-Rock Interactions in Gale Crater Inferred from Orbital and In-Situ Observations. Minerals 11, pp.986.

Stähler, S.C., Mittelholz, A., Perrin, C., Kawamura, T., Kim, D., Knapmeyer, M., Zenhäusern, G., Clinton, J., Giardini, D., Lognonné, P., Banerdt, W.B., 2022. Tectonics of Cerberus Fossae unveiled by marsquakes. Nat Astron 6, pp.1376–1386.

The Omega Team, Poulet, F., Bibring, J.-P., Mustard, J.F., Gendrin, A., Mangold, N., Langevin, Y., Arvidson, R.E., Gondet, B., Gomez, C., 2005. Phyllosilicates on Mars and implications for early martian climate. Nature 438, pp.623–627.

Tosca, N.J., Knoll, A.H., McLennan, S.M., 2008. Water Activity and the Challenge for Life on Early Mars. Science 320, pp.1204–1207.

Watkins, J.A., Ehlmann, B.L., Yin, A., 2020. Spatiotemporal evolution, mineralogical composition, and transport mechanisms of long-runout landslides in Valles Marineris, Mars. Icarus 350, pp.113836.

Wernicke, L.J., Jakosky, B.M., 2021. Martian Hydrated Minerals: A Significant Water Sink. JGR Planets 126, e2019JE006351.